A Planner for Autonomous Risk-Sensitive Coverage (PARCOV) by a Team of Unmanned Aerial Vehicles

Alex Wallar Erion Plaku Donald A. Sofge

***Abstract*— This paper proposes a path-planning approach to enable a team of unmanned aerial vehicles (UAVs) to efficiently conduct surveillance of sensitive areas. The proposed approach, termed PARCOV (Planner for Autonomous Risk-sensitive Coverage), seeks to maximize the area covered by the sensors mounted on each UAV while maintaining high sensor data quality and minimizing detection risk. PARCOV uses a dynamic grid to keep track of the parts of the space that have been surveyed and the times that they were last surveyed. This information is then used to move the UAVs toward areas that have not been covered in a long time. Moreover, a nonlinear optimization formulation is used to determine the altitude at which each UAV flies. The efficiency and scalability of PARCOV is demonstrated in simulation using complex environments and an increasing number of UAVs to conduct risk-sensitive surveillance.**

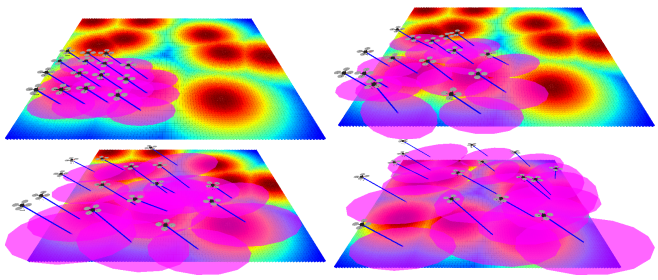

Fig. 1. Snapshots of PARCOV at different iterations showing how the quadcopters cover the designated area. The risk model is shown as a heatmap with red indicating high risk and blue indicating low risk. Figures better viewed in color and on screen.

I. INTRODUCTION

UAVs are seen as providing a viable way to enhance automation in environmental monitoring, search-and-rescue missions, package delivery, target tracking, and many other applications. UAVs, such as ARDrone and AscTec Pelican quadcopters, are becoming more commercially available, making them also an economically-feasible option for deployment in autonomous aerial missions.

Towards increasing the autonomy of UAVs, this paper describes an algorithm for persistent area coverage using multiple cooperative quadcopters while accounting for the risk and sensor data quality involved in the coverage. The proposed approach, PARCOV, seeks to move the quadcopters to promote informed coverage and adjusts the altitude to maximize sensor data quality while minimizing the associated risk. Risk plays an important role in many autonomous aerial missions, especially when seeking to reduce the likelihood of being detected by a possibly hostile agent. Although this paper focuses on detection risk, PARCOV is general and can minimize other risk metrics that decrease in value as the altitude increases. For instance, risk can also be used to model a brushfire. In such scenario, PARCOV can provide risk-sensitive aerial coverage of a wildfire while maximizing the sensor data quality.

There is a burgeoning body of work focusing on aerial missions using one or several UAVs [1], [2]. Ergezer and Leblebicioğlu [3] describe an algorithm for 3D path planning using UAVs that seeks to avoid forbidden regions and maximize information collection from desired regions. Nikolos et al. [4] develop evolutionary algorithms for offline/online path planning for UAVs. Kuhlman et al. [5] provide an algorithm that optimizes a closed-loop trajectory path for persistent area coverage by a single UAV that maximizes the information gained from information-rich areas. Beard and McLain [6] take into account communication-range constraints in order to ensure that UAVs always remain in communication range as they visit desired regions and avoid forbidden regions. Cheng, Keller, and Kumar [7] derive a control policy that generates time-optimal UAV trajectories for urban structure coverage. Chandler, Pachter, and Rasmussen [8] propose cooperative control techniques in order to minimize team exposure to radar detection. Distributed-task allocation procedures are developed in [9]–[11] in order to enhance cooperative searching. Sydney, Paley, and Sofge [12] provide a physicomimetic method for target detection using a group of UAVs. This approach continuously searches the area by following the gradient of an information surface to track targets using mutual information between the UAVs. A bio-inspired approach is proposed in [13] which seeks to model the information of a search space as a field for grazing and the UAVs as grazing animals that seek to eat the available information. This approach has shown to converge more quickly to total information collection than traditional lawnmower methods. Genetic algorithms are used in [14] to design evolving behaviors that could increase the autonomy of a swarm of UAVs in carrying out search-and-destroy missions. Huynh, Enright, and Frazzoli [15] analyze the persistent-patrol problem for a team of UAVs and propose several policies to minimize the expected waiting time between the occurrence and detection time of an incident.

The proposed approach, PARCOV, offers several contributions. In particular, it utilizes simple interactions between UAVs to promote an emergent behavior that maximizes

A. Wallar is with the School of Computer Science, University of St Andrews, Fife KY16 9AJ, Scotland, UK. E. Plaku is with the Dept. of Electrical Engineering and Computer Science, Catholic University of America, Washington DC 20064 USA. D. A. Sofge is with the Naval Research Laboratory, Washington, DC 20375 USA.

coverage and sensor data quality while minimizing the risk. PARCOV achieves scalability by separating planning of motions to maximize coverage with adjustments in altitude to account for sensor data quality and risk. PARCOV does not try to avoid forbidden regions, but seeks to mitigate the potential risk. The efficiency and scalability of PARCOV is demonstrated in 3D simulation using complex environments and an increasing number of UAVs to conduct surveillance.

II. PROBLEM FORMULATION

In the problem setting considered in this paper, a number of quadcopters are required to survey a given area. The coverage criteria and the models for sensor data quality and detection risk are described below.

a) Area coverage and persistency: Each quadcopter is equipped with a sensor which is mounted at a fixed angle ϕ. The team of quadcopters seeks to maximize the area coverage on the xy-plane, where a point is considered covered if it is sensed by at least one of the quadcopters. More specifically, the area covered by the quadcopters at time t is given by

$$\mathit{SensedArea}_{q_1}(t) \cup \ldots \cup \mathit{SensedArea}_{q_n}(t),$$

where n denotes the number of quadcopters and $\mathit{SensedArea}_{q_i}(t)$ denotes the area on the xy-plane sensed by the i-th quadcopter at time t. The experiments in this paper consider spotlight sensors, so the sensed area corresponds to an ellipse, which is a function of the position and orientation of the quadcopter, the angle ϕ at which the sensor is mounted, and the conic aperture α. Fig. 1 provides an illustration of the area covered by the quadcopters.

As the team of quadcopters may not be sufficiently large to achieve complete area coverage, another objective of PARCOV is to ensure that no part of the space goes too long without being surveyed. In this way, the quadcopters will not remain still but fly from one part to the next to ensure that the entire area is persistently surveyed.

b) Quality of sensor data: A second objective is to maintain high sensor data quality, which is needed in many applications in order to detect objects of interest in the area being surveyed. To model the quality of the sensor data, it is assumed first that there is an optimal altitude, denoted by μ_{sq}, to fly the quadcopter in order to achieve the highest sensor data quality. This optimal altitude depends on the object being tracked and varies from situation to situation. For example, the optimal altitude to track a person is much less than the optimal altitude to track a tank since the tank is larger and moves faster. In this paper, the optimal altitude μ_{sq} is passed to PARCOV as an argument by the user.

Furthermore, the sensor data quality is assumed to decrease exponentially as the deviation from the optimal altitude increases. More precisely, the sensor data quality is modeled as a distribution with mean μ_{sq} and standard deviation σ_{sq}, i.e.,

$$SQ(z) = \exp\left(-\left(\frac{z}{\cos\phi} - \mu_{sq}\right)^2/(2\sigma_{sq}^2)\right),$$

where z is the altitude at which the quadcopter is flying and ϕ is the angle at which the sensor is mounted.

c) Detection risk: While surveying the area, the quadcopters also seek to reduce the risk of being detected, where a function $R : \mathbb{R}^3 \rightarrow (0, 1)$ determines the detection risk $R(x, y, z)$ at each location (x, y, z). In this paper, $R(x, y, z)$ is modeled based on a ground-level risk, $R_0 : \mathbb{R}^2 \rightarrow (0, 1)$, where $R_0(x, y)$ indicates the risk of the quadcopter being detected at location (x, y) on the ground level. More specifically, the ground-level risk is used to scale R as altitude increases with an exponential decay, defined as follows:

$$R(x, y, z) = R_0(x, y) \cdot \exp\left(-\frac{z^2}{K \cdot R_0(x, y)^2}\right),$$

where K is a scaling constant. In this way, when the ground-level risk is high, which would indicate a hostile environment, the quadcopters would need to fly at high altitudes in order to reduce the detection risk. When the ground-level risk is low, the quadcopters can fly at lower altitudes without risking detection.

The ground-level risk $R_0(x, y)$ is modeled by centering normal distributions around risk points that are given a priori. More precisely, a set of risk points $\mathit{RiskPoints} = \{p_1, \ldots, p_m\}$ is sampled uniformly at random inside the boundaries of the area to be surveyed. Each risk point p_i defines a threat that decreases exponentially as the distance from p_i increases. Then, $R_0(x, y)$ is defined as

$$R_0(x, y) = \max_{p \in \mathit{RiskPoints}} \exp\left(-\frac{||p - (x, y)||_2}{L}\right),$$

where L is a scaling constant. An illustration of $R_0(x, y)$ is provided in Fig. 2.

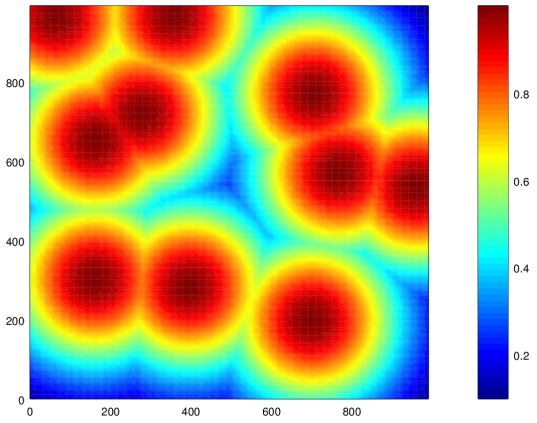

Fig. 2. Illustration of the ground-level risk $R_0(x, y)$ corresponding to the case of 10 randomly-sampled risk points. Color intensity indicates risk values.

d) Problem statement: Putting it all together, the problem considered in this paper can be stated as follows: Given an area to be surveyed, models for sensor data quality and detection risk, and an initial placement of the quadcopters, move the quadcopters so that they maximize area coverage, ensure that no part of the space goes too long without being surveyed, maintain high sensor data quality, and reduce the detection risk.

III. METHOD

To achieve the stated objectives, PARCOV splits planning into two stages: (i) planning the quadcopters' motions in xy to promote area coverage and persistency and (ii) planning for the altitude to minimize the detection risk and maximize sensor data quality. Pseudocode is provided in Alg. 1. Descriptions of the main steps of the algorithm follow.

Algorithm 1 Pseudocode for PARCOV

1: $\mathcal{G} \leftarrow$ INITGRID()
2: **while** FINISHED() $=$ `false` **do**
3: **for** $q \in$ *Quadcopters* **do**
4: $(v', \beta') \leftarrow$ GETDIRECTIONANDORIENTATION$(q, \mathcal{G})$
5: $\begin{bmatrix} x' \\ y' \end{bmatrix} \leftarrow \begin{bmatrix} q.x \\ q.y \end{bmatrix} + \mathit{step} \cdot \frac{v'}{||v'||}$
6: $z' \leftarrow$ DETERMINEALTITUDE(x', y')
7: SETPOSITIONANDORIENTATION(q, x', y', z', β')
8: UPDATEGRID$(\mathcal{G}, q)$

A. Planning to promote area coverage and persistency

First, PARCOV imposes a grid over the xy bounding box of the area being surveyed. The grid, denoted by $\mathcal{G}$, is used to keep track of the parts of the space that have been surveyed and the times that they were last surveyed (Alg. 1:1). Whenever a grid cell c is sensed by some quadcopter, i.e., $c \in \mathit{SensedArea}_{q_i}(t)$, the current time t is stored in that grid cell (Alg. 1:8). An illustration of the grid $\mathcal{G}$ at some time instance is provided in Fig. 3.

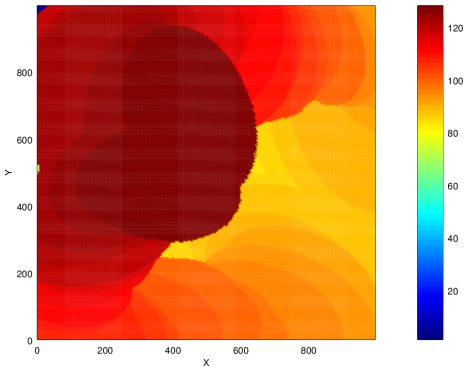

Fig. 3. An instance of the grid $\mathcal{G}$ where the color in the spectrum denotes the time (as iteration count) that the cell at x, y was visited, i.e., red denotes recently-visited areas.

PARCOV uses the grid $\mathcal{G}$ to determine the new direction and orientation of each quadcopter. Pseudocode is given in Alg. 2. In particular, PARCOV seeks to move a quadcopter q toward areas that have not been covered in a long time. In order to take advantage of locality, PARCOV considers the vicinity of the area sensed by q at the current time.

To determine the new direction and new orientation, PARCOV first uses random sampling to generate a set of candidate orientations (Alg. 2:2). Let $\mathit{SensedArea}(\beta)$ denote the area that would be sensed by q when setting its orientation to β (keeping the position fixed). As an example, for the spotlight sensor model used in the experiments, the sensed area would be an ellipse defined parameterically with respect to $\omega \in [0, 2\pi]$ as follows:

$$\begin{bmatrix} x \\ y \end{bmatrix} + \mathit{Rot}(\beta) \cdot \begin{bmatrix} z \cdot \tan(\phi - \alpha) + A_M \cdot (1 + \cos\omega) \\ A_m \cdot \sin\omega \end{bmatrix},$$

where (x, y, z) is the position of the quadcopter, $\mathit{Rot}(\beta)$ is the 2D-rotation matrix, $A_M = z \cdot \tan(\phi + \alpha) - z \cdot \tan\phi$ is the major axis, and $A_m = \frac{z \cdot \tan\alpha}{\cos\phi}$ is the minor axis.

Next, PARCOV generates a number of segments along $\xi(\beta)$, where $\xi(\beta)$ denotes $\mathit{SensedArea}(\beta)$ enlarged by some $\epsilon > 0$ (Alg. 2:4–5). The i-th segment is generated by connecting the points on the perimeter of $\xi(\beta)$ corresponding to the angles $(i-1)\zeta$ and $(i+1)\zeta$, where ζ is a user-defined parameter (set to 10°). The average wait time for a segment s, denoted by $\mathit{AvgWaitTime}(\mathcal{G}, s)$, is computed by considering a number of equally-spaced points along the segment s, where $\mathit{WaitTime}(\mathcal{G}, x, y)$ denotes the number of iterations that have passed since the point (x, y) was last sensed by some quadcopter. Note that this information is obtained from the grid $\mathcal{G}$ by looking up the iteration number associated with the grid cell that contains (x, y) and subtracting the value of the grid cell from the current iteration number.

The quadcopter q will move toward the segment s with the maximum average wait time, i.e.,

$$s = \underset{s' \in \mathit{AllSegments}}{\arg\max} \; \mathit{AvgWaitTime}(\mathcal{G}, s')$$

where $\mathit{AllSegments} = \bigcup_{\beta \in \mathit{orientations}} \mathit{segments}(\xi(\beta))$. The new orientation of the quadcopter q is set to the candidate orientation β from which the $\xi(\beta)$ that contains the segment s was derived (Alg. 2:11). The new direction is set by taking a weighted average of the equally-spaced points along the segment s (Alg. 2:12–13), i.e.,

$$-(q.x, q.y) + \sum_{(x,y) \in \mathit{points}(s)} \frac{\mathit{WaitTime}(\mathcal{G}, x, y)}{t}(x, y),$$

where $t = \sum_{(x',y') \in \mathit{points}(s)} \mathit{WaitTime}(\mathcal{G}, x', y')$.

This rule has desirable emergent properties for the team of quadcopters. Since the quadcopters share the same grid $\mathcal{G}$, they will act cooperatively to fill the unvisited space without having to explicitly coordinate with one another. In particular, each quadcopter will move towards an area in its vicinity that has a large average wait time. This makes it less likely for the quadcopters to clutter together. Suppose two or more quadcopters are moving towards the same segment. When a quadcopter senses the segment, its wait time becomes zero, which causes the other quadcopters to move towards other segments. Furthermore, since the segment selected by each quadcopter q is in the vicinity of the area sensed by q, then it is likely that q will reach it first, hence further reducing the likelihood of clutter.

Moreover, this planning is not dependent on the number of quadcopters. If a quadcopter leaves the area, it would simply no longer update the grid $\mathcal{G}$. The other quadcopters would have no knowledge that it left and would still be able to persistently cover the area being surveyed. This is

Algorithm 2 GETDIRECTIONANDORIENTATION$(q, \mathcal{G})$

1: $\mathit{waitTime} \leftarrow -\infty; v' \leftarrow (0,0); \beta' \leftarrow 0$
2: $\mathit{orientations} \leftarrow$ GETRANDOMSAMPLES$(0, 2\pi)$
3: **for** $\beta \in \mathit{orientations}$ **do**
4: $\quad \xi \leftarrow$ ENLARGEDELLIPSE$(q.x, q.y, q.z, \beta, \phi, \alpha, \epsilon)$
5: $\quad \mathit{segments} \leftarrow$ GETSEGMENTS(ξ)
6: $\quad$ **for** $s \in \mathit{segments}$ **do**
7: $\quad\quad \mathit{points} \leftarrow$ GETPOINTS(s)
8: $\quad\quad t \leftarrow \sum_{(x,y)\in \mathit{points}} \mathit{WaitTime}(\mathcal{G}, x, y)$
9: $\quad\quad$ **if** $\mathit{waitTime} < t/|\mathit{points}|$ **then**
10: $\quad\quad\quad \mathit{waitTime} \leftarrow t/|\mathit{points}|$
11: $\quad\quad\quad \beta' \leftarrow \beta$
12: $\quad\quad\quad (\bar{x}, \bar{y}) \leftarrow \sum_{(x,y)\in \mathit{points}} \frac{\mathit{WaitTime}(\mathcal{G},x,y)}{t} \cdot (x, y)$
13: $\quad\quad\quad v' \leftarrow (\bar{x} - q.x, \bar{y} - q.y)$
14: $\quad$ **return** (v', β')

particularly important for missions that combine persistent coverage and target tracking. The persistent coverage can be used to determine the positions of targets, and a sub-swarm of quadcopters can be deployed from the group to track the targets while the rest continues to provide coverage.

B. Determining the altitude

To determine the altitude, PARCOV optimizes an objective function that maximizes the sensor data quality and minimizes the detection risk, i.e.,

$$J(x, y, z) = SQ(z) - R(x, y, z).$$

Therefore, the optimal altitude can be determined by finding the z value that maximizes J for a given x, y, i.e.,

$$\text{DETERMINEALTITUDE}(x, y) = \underset{z\in[z_{min}, z_{max}]}{\arg\max} \; J(x, y, z).$$

Nonlinear optimization solvers can then be used to numerically compute the optimal altitude (this paper uses SciPy, which is open source).

After determining the altitude, the quadcopter is set at the new position and orientation (Alg. 1:18). The grid is updated accordingly to account for the new sensed area. Since the grid is shared among the quadcopters, the change in altitude of one quadcopter would cause a change in the sensed area, which could potentially change which parts of the grid are covered. As a result, the rest of the group will react to this new information. In particular, if a quadcopter decreases its altitude, then there will be more uncovered space around it so the rest of the quadcopters will move to cover this space. These dynamic adjustments, as shown by the experimental results, make it possible to efficiently and persistently cover the area being surveyed while maintaining high sensor data quality and reducing the detection risk.

IV. EXPERIMENTS AND RESULTS

Experiments are conducted in simulation with an increasing number of quadcopters and risk points.

A. Experimental Setup

1) Scenes: A scene is defined by its dimensions and the number and location of the risk points. Three scene dimensions were used: small ($600 \times 600 \times 160$), medium ($1000 \times 1000 \times 160$), and large ($2000 \times 2000 \times 160$). The risk points were randomly placed inside the xy bounding box. The generated scenes are referred to as *sceneX_n*, where $X \in \{\mathit{small}, \mathit{medium}, \mathit{large}\}$, and $n \in \{1, 3, 5, \ldots, 21\}$. The quadcopters all started in a square formation at the top left of the scene. The number of quadcopters was varied as $1, 6, 11, 16, 21, 26$.

2) Performance criteria: Results report on the average percentage of the total area coverage, the average sensor data quality, the average risk, and average wait time in the grid $\mathcal{G}$. The sensor data quality and risk metrics were determined using the same functions as in the optimization process (Section II).

Area coverage was computed using a Monte-Carlo process where a large number of random points (1000) were sampled inside the xy bounding box of the scene. At each iteration of PARCOV, each sampled point is checked whether or not it is sensed by some quadcopter. The ratio of the number of sampled points which are within any of the sensed areas to the total number of sampled points was used to determine the percentage of the total area covered.

The average wait time is used to show that no part of the area being surveyed goes for too long a time without being sensed. This metric was computed at each iteration as

$$\frac{1}{|\mathit{cells}(\mathcal{G})|} \sum_{c\in \mathit{cells}(\mathcal{G})} \mathit{WaitTime}(\mathcal{G}, c).$$

Recall that $\mathit{WaitTime}(\mathcal{G}, c)$ corresponds to the number of iterations since the last time c was sensed by some quadcopter.

3) Hardware and software: Experiments are conducted on an Intel Core i7 machine (CPU: 2.40GHz, RAM: 16GB) using Ubuntu 14.04. Code was written in Python 2.7. ROS rviz was used for visualization.

B. Results

Before presenting quantitative results, we provide some qualitative illustrations to show PARCOV in action. Fig. 1 shows how the quadcopters cover the designated area. Using the information from the grid $\mathcal{G}$, the quadcopters start moving toward the uncovered areas.

Another illustration of PARCOV in action is provided in Fig. 4, which shows trajectories taken by two quadcopters. Note how the quadcopters increase their altitude when surveying areas designated as high risk and reduce their altitude when going over low-risk areas. As discussed in Section III-B, PARCOV uses a nonlinear optimization process to reduce detection risk while maintaining high sensor data quality.

1) Performance as a function of the number of iterations: Fig. 6 shows that in a small number of iterations, regardless of the number quadcopters or number of risk points, the team of quadcopters was able to achieve high coverage of the designated area. In fact, at around 20 iterations the coverage was

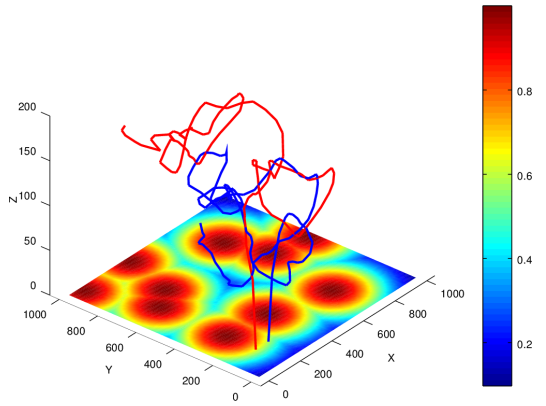

Fig. 4. Trajectories taken by two quadcopters shown in blue and red, respectively. The initial risk R_0 is shown as a heatmap (a different color scheme is used here to better visualize the trajectories).

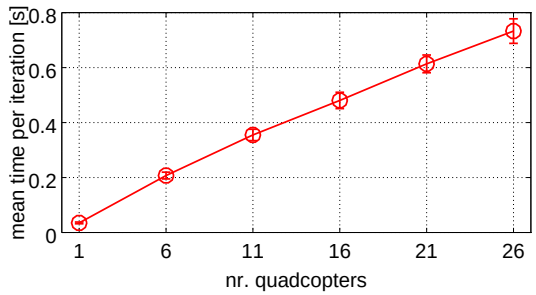

Fig. 5. Runtime per iteration. Bars indicate standard deviation.

over 90% for each of the scenarios. An iteration corresponds to computing one move (position and orientation) for each quadcopter (Alg. 1:4–8). As shown in Fig. 5, PARCOV scales linearly with the number of quadcopters.

Results in Fig. 6 also show that the detection risk rapidly decreased. To test the ability of the approach to reduce the detection risk, in the experiments the quadcopters started at the minimum viable height, which carries the highest risk. The quadcopters were quickly able to readjust their height to minimize the risk. Likewise, the sensor data quality rapidly increased as the iterations increased because the quadcopters quickly determined the optimal altitude. We also notice that the sensor data quality, coverage, and detection risk did not change much as the number of risk points increased. This is because the quadcopters are able to spread out appropriately and reconfigure the altitude in order to maximize the sensor data quality and minimize the detection risk.

2) Performance as a function of the number of quadcopters: Results in Fig. 7 show the performance criteria as the number of quadcopters is increased. As expected, the area coverage increases as more quadcopters participate in the task. The increase in coverage is very rapid initially and slows down as the required number of quadcopters to ensure complete coverage is reached. These results indicate that PARCOV effectively dispatches the quadcopters to fly over uncovered areas. Moreover, PARCOV keeps the detection risk low and the sensor quality high even as the number of quadcopters is increased. The same trends are observed

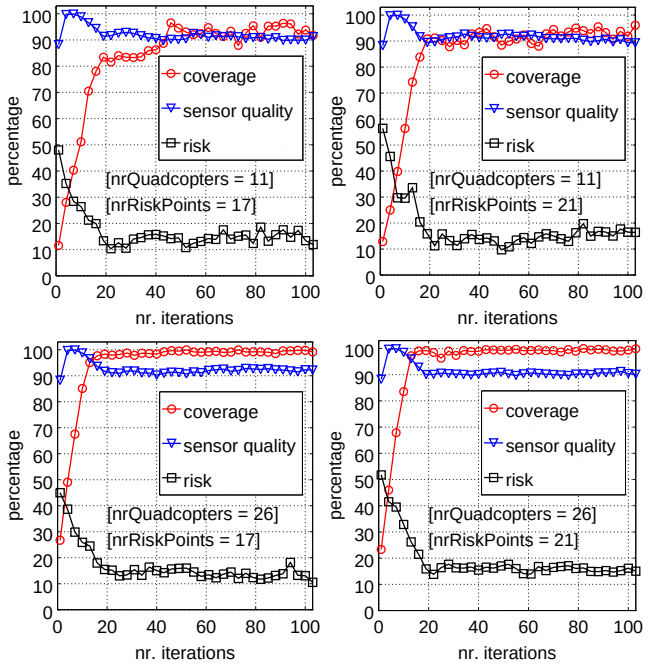

Fig. 6. Performance criteria as a function of the number of iterations. Results are shown for instances of the medium-size scene with different numbers of risk points and quadcopters.

even when increasing the number of risk points (Fig. 7 plots the performance criteria as a function of the number of quadcopters for three different scenarios obtained by varying the number of risk points).

3) Wait times: Table I shows the average wait time (Section IV-A.2) as a function of the number of quadcopters. As the number of quadcopters increases, the average wait time decreases since the quadcopters spread through the space cooperatively and therefore cover the space more quickly.

nr. quadcopters	1	6	11	16	21	26
awt [nrRiskPts=13]	37.90	2.19	0.14	0.08	0.03	0.03
awt [nrRiskPts=17]	37.14	3.09	0.18	0.12	0.06	0.04
awt [nrRiskPts=21]	35.53	1.89	0.19	0.11	0.06	0.02

TABLE I
AVERAGE WAIT TIME (AWT).

4) Performance as a function of scene size: Table II shows the performance of PARCOV on three different scene sizes: small, medium, and large. In all cases, PARCOV efficiently covers the area while maintaining high-sensor quality and low detection risk. As expected, more quadcopters are needed to cover the large scene.

5) Performance as a function of the projection angle: Fig. 8 provides a summary of the results when varying the angle ϕ at which the sensor is attached to the quadcopter. As shown, PARCOV works well for a variety of values.

V. DISCUSSION

This paper developed a path-planning approach to enable a team of quadcopters to efficiently conduct surveillance.

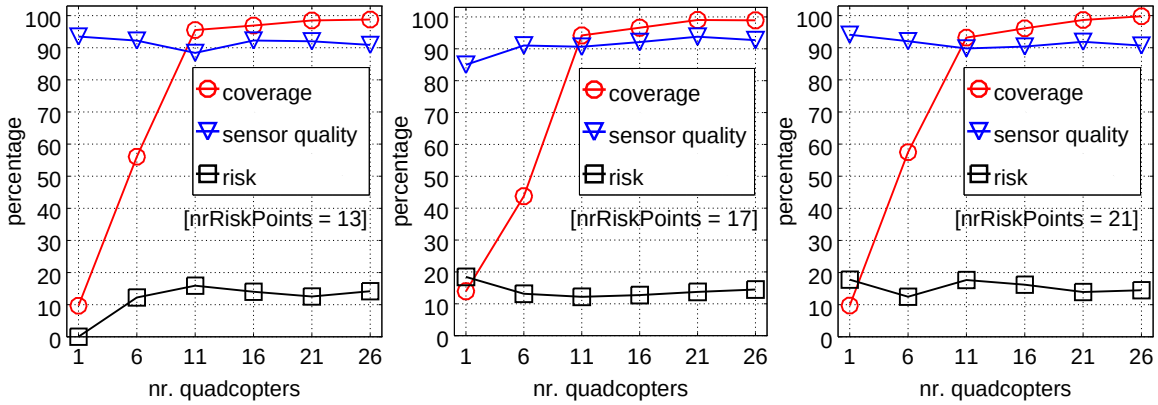

Fig. 7. Performance criteria as a function of the number of quadcopters. Shown percentages are computed after 250 iterations of the algorithm. Results are shown for instances of the medium-size scene with different numbers of risk points.

nr. quadcopters	1	6	11	16	21	26	30	35
(A) coverage	51%	95%	98%	99%	99%	99%	99%	99%
(B) coverage	13%	43%	94%	96%	99%	99%	99%	99%
(C) coverage	3%	26%	44%	54%	62%	77%	84%	93%
(A) sensor quality	88%	92%	92%	92%	91%	92%	92%	92%
(B) sensor quality	84%	91%	90%	92%	93%	92%	92%	92%
(C) sensor quality	90%	90%	89%	91%	89%	90%	89%	90%
(A) risk	27%	12%	13%	14%	15%	15%	15%	15%
(B) risk	18%	13%	12%	12%	13%	14%	14%	14%
(C) risk	15%	16%	19%	14%	16%	15%	16%	15%

TABLE II

(A) SMALL SCENE: 600X600X200 (B) MEDIUM SCENE: 1000X1000X200 (C) LARGE SCENE: 2000X2000X200. IN ALL CASES, NRRISKPTS=17.

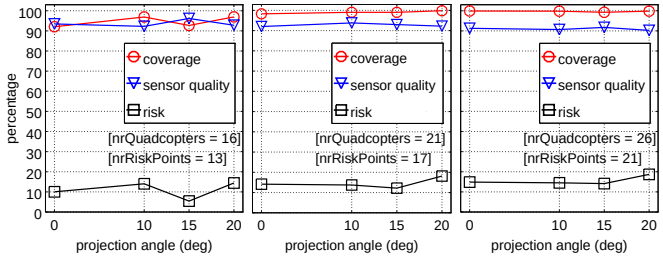

Fig. 8. Performance criteria as function of the angle at which the sensor is attached to the quadcopter. Shown percentages are computed after 250 iterations of the algorithm. Results are shown for the medium-size scene with different numbers of risk points and quadcopters.

PARCOV achieved scalability by separating planning of motions to maximize coverage with adjustments in altitude to account for sensor data quality and detection risk. The efficiency and scalability of PARCOV was demonstrated in simulation using complex environments and an increasing number of UAVs to conduct surveillance. In future work, we will enhance the approach to track moving targets. Another direction for future research is to further improve the sensor quality by reducing the motion blur. We are also working on using the approach on a team of ARDrone and AscTec Pelican quadcopters. In order to execute the planned motions, the approach will be complemented with PD controllers.

ACKNOWLEDGMENT

This work was performed at the Naval Research Laboratory and was funded by the US Department of Defense, Office of Naval Research under grant number N0001413WX21045, "Mobile Autonomous Teams for Navy Information Surveillance and Search (MANTISS)." The views, positions and conclusions expressed herein reflect only the authors opinions and expressly do not reflect those of the US Department of Defense, Office of Naval Research, or the Naval Research Laboratory.

REFERENCES

[1] A. Ryan, M. Zennaro, A. Howell, R. Sengupta, and J. K. Hedrick, "An overview of emerging results in cooperative UAV control," in *IEEE Conference on Decision and Control*, vol. 1, 2004, pp. 602–607.

[2] C. Goerzen, Z. Kong, and B. Mettler, "A survey of motion planning algorithms from the perspective of autonomous uav guidance," *Journal of Intelligent and Robotic Systems*, vol. 57, no. 1-4, pp. 65–100, 2010.

[3] H. Ergezer and K. Leblebicioğlu, "3D path planning for multiple UAVs for maximum information collection," *Journal of Intelligent & Robotic Systems*, vol. 73, no. 1-4, pp. 737–762, 2014.

[4] I. K. Nikolos, K. P. Valavanis, N. C. Tsourveloudis, and A. N. Kostaras, "Evolutionary algorithm based offline/online path planner for uav navigation," *IEEE Transactions on Systems, Man, and Cybernetics, Part B: Cybernetics*, vol. 33, no. 6, pp. 898–912, 2003.

[5] M. J. Kuhlman, P. Svec, K. N. Kaipa, D. Sofge, and S. K. Gupta, "Physics-aware informative coverage planning for autonmous vehicles," in *IEEE International Conference on Robotics and Automation*, 2014, in press.

[6] R. W. Beard and T. W. McLain, "Multiple UAV cooperative search under collision avoidance and limited range communication constraints," in *IEEE Conference on Decision and Control*, vol. 1, 2003, pp. 25–30.

[7] P. Cheng, J. Keller, and V. Kumar, "Time-optimal UAV trajectory planning for 3d urban structure coverage," in *IEEE/RSJ International Conference on Intelligent Robots and Systems*, 2008, pp. 2750–2757.

[8] P. R. Chandler, M. Pachter, and S. Rasmussen, "UAV cooperative control," in *IEEE American Control Conference*, vol. 1, 2001, pp. 50–55.

[9] I. Maza and A. Ollero, "Multiple UAV cooperative searching operation using polygon area decomposition and efficient coverage algorithms," in *Distributed Autonomous Robotic Systems 6*. Springer, 2007, pp. 221–230.

[10] Y. Jin, A. A. Minai, and M. M. Polycarpou, "Cooperative real-time search and task allocation in uav teams," in *IEEE Conference on Decision and Control*, vol. 1, 2003, pp. 7–12.

[11] T. Lemaire, R. Alami, and S. Lacroix, "A distributed tasks allocation scheme in multi-uav context," in *IEEE International Conference on Robotics and Automation*, vol. 4, 2004, pp. 3622–3627.

[12] N. Sydney, D. A. Paley, and D. Sofge, "Physics-inspired robotic motion planning for cooperative bayesian target detection," in *Robotics: Science and Systems*, 2014, workshop on Distributed Control and Estimation for Robotic Vehicle Networks.

[13] T. Apker, S.-Y. Liu, D. Sofge, and J. K. Hendrick, "Application of grazing-inspired guidance laws to autonomous information gathering," in *IEEE/RSJ International Conference on Intelligent Robots and Systems*, 2014, in press.

[14] P. Gaudiano, E. Bonabeau, and B. Shargel, "Evolving behaviors for a swarm of unmanned air vehicles," in *IEEE Swarm Intelligence Symposium*, 2005, pp. 317–324.

[15] V. A. Huynh, J. J. Enright, and E. Frazzoli, "Persistent patrol with limited-range on-board sensors," in *IEEE Conference on Decision and Control*, 2010, pp. 7661–7668.